

Raman study of Twin Free $\text{YBa}_2\text{Cu}_3\text{O}_{6.5}$ (Ortho-II) Single Crystals

M. N. Iliev, V. G. Hadjiev

*Texas Center for Superconductivity,
University of Houston, Texas 77204-5002, USA*

S. Jandl, D. Le Boeuf

*Regroupement Québécois sur les Matériaux de Pointe, Département de Physique,
Université de Sherbrooke, Sherbrooke, Canada J1K 2R1*

V. N. Popov

Faculty of Physics, University of Sofia, 1164 Sofia, Bulgaria

D. Bonn, R. Liang, W. N. Hardy

*Department of Physics and Astronomy,
University of British Columbia, Vancouver, BC, Canada V6T 1Z1*

(Dated: November 29, 2018)

Abstract

The polarized Raman scattering spectra from freshly cleaved ab , ac , and bc surfaces of high quality twin free $\text{YBa}_2\text{Cu}_3\text{O}_{6.5}$ (Ortho-II) single crystals ($T_c=57.5$ K and $\Delta T = 0.6$ K) were studied between 80 and 300 K. All eleven A_g Raman modes expected for the Ortho-II structure as well some modes of B_{2g} and B_{3g} symmetry were identified in close comparison with predictions of lattice dynamical calculations. The electronic scattering from the ab planes is strongly anisotropic and decreases between 200 and 100 K within the temperature range of previously reported pseudogap opening. The coupling of phonons to Raman active electronic excitations manifested by asymmetric (Fano) profiles of several modes also decreases in the same range. Among the new findings that distinguish the Raman scattering of Ortho-II from that of Ortho-I phase is the unusual relationship ($\alpha_{xx} \approx -\alpha_{yy}$) between the elements of the Raman tensor of the apex oxygen A_g mode.

PACS numbers: 78.30.-j, 74.25.Kc, 74.72.Bk

I. INTRODUCTION

The properties of underdoped $\text{YBa}_2\text{Cu}_3\text{O}_x$ ($6 < x < 7$) have been studied intensively within the efforts to unravel the mechanism of high temperature superconductivity. The Ortho II phase, corresponding to oxygen content $x = 6.5$ and characterized by alternating full and empty chains, has attracted particular attention as it is both underdoped and free of disorder. Although the existence of this phase has been documented experimentally in considerable number of reports, it has also been established that as a rule the Ortho II domains coexists with domains of different oxygen ordering or/and strong disorder even in the case $x \simeq 6.5$. An improved procedure developed by Liang et al.[1] has made possible preparation of twin free, highly ordered Ortho II single crystals. Such crystals have recently been used in several studies of specific properties of the Ortho II phase by means of neutron scattering[2, 3], x-ray diffraction[4], time-resolved spectroscopy[5, 6], infrared spectroscopy[7], nuclear magnetic resonance[8], microwave spectroscopy[9], and resistance measurements in high magnetic fields.[10].

There have been several attempts to identify the Raman modes of the Ortho-II phase by measuring the spectra of oxygen deficient $\text{YBa}_2\text{Cu}_3\text{O}_x$ ($x \approx 6.5$) single crystals.[11, 12, 13] Compared to the well known Raman spectra of Ortho-I ($x = 7$) and T ($x = 6$) phases, in the case of Ortho-II one expects shift of the corresponding Raman modes and activation of additional modes due to the doubling of the unit cell. A significant number of additional modes have been observed, but their identification has met definite difficulties due to ambiguities in the local structure of $\text{YBa}_2\text{Cu}_3\text{O}_x$ even in the case $x = 6.5$. Indeed, in the idealized Ortho-I, Ortho-II and T structures the Cu1 and O1 atoms in the basal Cu-O planes are at centrosymmetrical sites and their vibrations are not Raman active. The oxygen arrangement in the basal planes of a real $\text{YBa}_2\text{Cu}_3\text{O}_x$ material, however, is characterized by chain fragments instead of infinite chains and part of oxygen atoms are outside the chains in otherwise vacant O5 sites. This creates a number of local non-centrosymmetrical surroundings for Cu and O atom, in particular those at the end of chain fragments, and activates their vibrations in the Raman spectrum.[13, 14] Some of these defects can also be produced by local laser annealing[15, 16] or photoactivation.[17] Another issue, as a rule neglected but of particular importance in the case of Ortho-II phase, is the possible lack of correspondence between the oxygen content and arrangement in the volume of the crystal

and its surface layer(s), where the Raman scattering occurs. The cause for such discrepancy is the in- and out-diffusion of oxygen, which depends strongly on the type of the surface (ab , bc or ac), starting oxygen content, ambient oxygen pressure, temperature and exposure time.[22]

In this paper we present results of a temperature-dependent Raman study on freshly-cleaved ab , ac , and bc surfaces of a twin free $\text{YBa}_2\text{Cu}_3\text{O}_{6.5}$ (YBCO6.5) single crystal with high degree of Ortho-II type ordering. This allowed us with great certainty to identify the proper Raman modes of the Ortho-II phase and assign them to definite atomic motions via close comparison with predictions of lattice dynamical calculations, as well as to measure the symmetry and strength of electronic scattering.

II. SAMPLES AND EXPERIMENTAL

We used a high quality mechanically de-twinned Ortho-II YBCO6.5 single crystal with $T_c=57.5$ K and $\Delta T = 0.6$ K, grown by a flux method in BaZrO₃ crucible.[1, 10] Immediately before mounting the sample on the cold finger of a Microstat®He (Oxford Instruments) optical cryostat, a small area of the surface (ab , ac , or bc) to be used for Raman measurements was cleaved out to ensure that the scattering volume has an Ortho-II oxygen arrangement. The Raman spectra were measured under microscope ($\times 50$ magnification) using a triple T64000 (Horiba Jobin Yvon) spectrometer. In most experiments we used 633 nm excitation with less than 1 mW incident laser power focused at a spot of 2-3 μm diameter. Comparative measurements with 515, 488, and 458 nm excitations were also done. All spectra were corrected for the Bose factor. For description of the scattering configurations we use the Porto's notation $a(BC)d$, where the first and fourth letters denote, respectively, the directions of incident and scattered light in a Cartesian xyz system with axes along the crystallographic directions. The polarization of the incident and scattered light is given by the second and third letters, respectively.

III. RESULTS AND DISCUSSION

A. Raman phonons in the Ortho-II phase

In Figure 1 are compared the Raman spectra obtained with 633 nm excitation at room temperature from freshly cleaved and aged areas on the ab and bc surfaces of the same Ortho-II crystal. The spectral shapes and Raman line frequencies from aged surfaces are consistent with those from earlier reports on the XX/YY and ZZ spectra of twinned YBCO_{6.5}[12] and YBCO x ($x \approx 6.5$ samples.[19, 20] The corresponding spectra from freshly cleaved and aged surfaces, however, exhibit definite differences in the positions and appearance of some of the peaks.

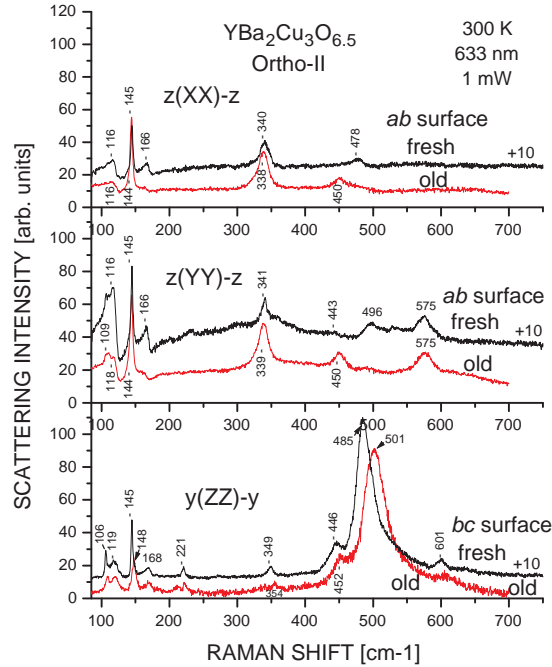


FIG. 1: (Color online) Raman spectra of YBa₂Cu₃O_{6.5} (Ortho-II) obtained from freshly cleaved and aged ab and bc surfaces.

Figure 2 shows the Raman spectra from freshly cleaved surfaces at 90 K in all available exact scattering configurations. From symmetry considerations one expects for the Ortho-II structure an increased number of Raman active modes, $11A_g + 4B_{1g} + 11B_{2g} + 8B_{3g}$, compared to the $5A_g + 5B_{2g} + 5B_{3g}$ modes of the Ortho-I structure. The atomic displacements of the

eleven A_g modes, as predicted by lattice dynamical calculations, (LDC)[13] are shown in Figure 3. For most modes, the experimentally observed frequencies (at 90 K) are in good agreement with those predicted by LDC, shown in parenthesis. In addition to the five A_g modes at 126, 147, 342, 447, and 487 cm^{-1} corresponding to displacements along the c -axis of Ba, Cu2, O2-O3, O2+O3, O4 in the Ortho-I structure, there are six more A_g modes in the extended Ortho-II cell. Four of them can be positively identified at 107 cm^{-1} [Cu2(z)-Cu2'($-z$) out-of-phase], 171 cm^{-1} [Y(x)], 352 cm^{-1} [O4(z)-O4'($-z$) out-of-phase], and 579 cm^{-1} [O2(x)]. The mixed Ba/Cu mode, predicted at 146 cm^{-1} , may be very weak and not observable. The weak Raman line at 381 cm^{-1} can be tentatively assigned to the mode involving mainly O4' displacements along c , with a predicted frequency of 414 cm^{-1} . In the ZZ spectra one observes additional lines of A_g character at 224 and 601 cm^{-1} . These positions are close to those of defect modes related to displacements of Cu1 and O1 at the end of broken chains,[13, 15, 20] which could preexist or be created by photoactivation in our Ortho-II sample.

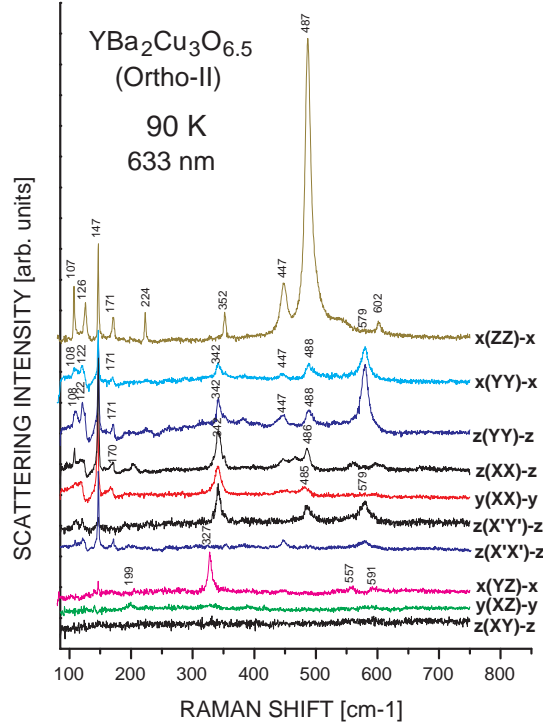


FIG. 2: (Color online) Raman spectra of $\text{YBa}_2\text{Cu}_3\text{O}_{6.5}$ (Ortho-II) obtained at 90 K from freshly cleaved ab , ac and bc surfaces. The spectra are shifted vertically for clarity.

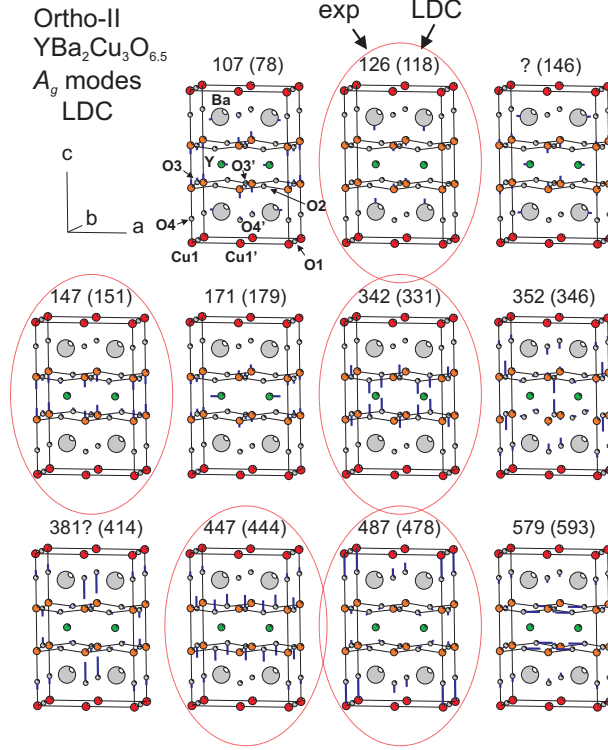


FIG. 3: (Color online) Main atomic displacements of the A_g modes of $\text{YBa}_2\text{Cu}_3\text{O}_{6.5}$ (Ortho-II) as obtained by LDC. The LDC predicted frequencies (in parenthesis) are compared to experimentally obtained values.

In the $XZ(B_{2g})$ and $YZ(B_{3g})$ spectra one observes relatively strong Raman peaks at 199 and 327 cm^{-1} , respectively. The closest B_{2g} (200 and 213 cm^{-1}) and B_{3g} (300 cm^{-1}) frequencies predicted by LDC, correspond to modes involving mainly displacements of O4 and O4' along a and b directions, respectively.

A more careful look at the appearance of the apex oxygen mode near 487 cm^{-1} in the $X'X'$ and $X'Y'$ spectra of Fig. 2 reveals a significantly different behavior compared to that in the corresponding spectra of the Ortho-I phase. Indeed, with these scattering configurations, the intensity of an A_g Raman line is proportional to $(\alpha_{xx} + \alpha_{yy})^2$ and $(\alpha_{xx} - \alpha_{yy})^2$, respectively, where α_{xx} and α_{yy} are diagonal elements of the corresponding Raman tensors. Negligible intensity in the $X'X'$ spectra may be expected if $\alpha_{xx} \approx -\alpha_{yy}$, which in the Ortho-I phase is satisfied only for the out-of-phase O2-O3 mode at $\approx 336 \text{ cm}^{-1}$, but not for the apex oxygen mode near 500 cm^{-1} (seen in the $X'X'$ but not in the $X'Y'$ spectrum). Here, for the Ortho-II phase the apex oxygen mode has an appearance similar to that of the out-of-phase mode: it is practically not seen in the $X'X'$ spectrum, but well pronounced in the $X'Y'$

spectrum with an intensity comparable to that in the XX and YY spectra. This allows us to conclude that for the apex oxygen mode of the Ortho-II phase, the relation $\alpha_{xx} \approx -\alpha_{yy}$ is satisfied.

B. Electronic scattering and electron-phonon interaction

In addition to discrete phonon lines, the Raman spectra of Ortho-II phase contain structureless background with intensity stronger with YY than with XX , and negligible intensity with ZZ polarization (Fig.4). Such background scattering, observed in the normal and superconducting states of high T_c superconductors has been attributed to electronic scattering and has been intensively studied both experimentally and theoretically.[23, 24, 25, 26] It has been shown that for optimally doped YBCO the electronic scattering is practically independent of temperature for $T > T_c$. With the opening of a superconducting gap Δ at $T < T_c$, there is a redistribution of electronic scattering intensity from lower to higher energies and a maximum associated with pair-breaking is formed at $\omega_{max} = 2\Delta$. For underdoped YBCO a slight decrease of electronic scattering intensity at $\omega < 600 \text{ cm}^{-1}$ has been observed below a characteristic temperature T^* well above T_c and this has been considered a manifestation of a pseudogap opening.[25] There are to our knowledge no reports on the variation of electronic scattering near T^* .

With few exceptions,[23, 27] in experimental studies of the electronic scattering in YBCO, twinned samples have been used and the theoretical models are based on the tetragonal approximation for the crystal structure.

Figs. 4 and 5 illustrate that the electronic scattering from the ab surface of the Ortho-II crystal is strongly anisotropic and temperature dependent below 600 cm^{-1} . Its intensity in the $z(YY)\bar{z}$ spectra is stronger by a factor 2 than in the $z(XX)\bar{z}$ and much stronger than in the $z(XY)\bar{z}$, $z(X'Y')\bar{z}$, $x(ZZ)\bar{x}$, and $x(YZ)\bar{x}$ spectra. We attribute the stronger electronic Raman intensity for YY polarization to the additional scattering channels involving two CuO_2 planar and a CuO chain bands crossing the Fermi surface along the $\Gamma(0,0,0) - Y(0,\pi,0)$ direction[28] in the Brillouin zone .

The coupling of the phonons to the electronic excitations contributing to the Raman background is manifested in our spectra by the asymmetric Fano profile of some of the A_g phonon lines, most clearly pronounced for these near 118 cm^{-1} (Ba), 168 cm^{-1} (Y) and

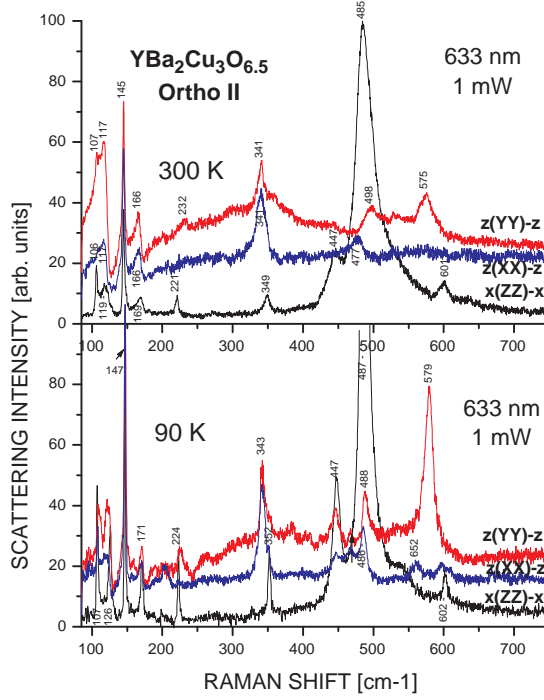


FIG. 4: (Color online) $z(XX)\bar{z}$, $z(YY)\bar{z}$, and $y(ZZ)\bar{y}$ spectra of Ortho-II at 300 and 90 K. Note the asymmetric Fano shape of the Ba(117 cm^{-1}), Y(166 cm^{-1}), and apex oxygen(477 and 498 cm^{-1}) modes in the XX and YY spectra at 300 K.

486 cm^{-1} (apex oxygen), which interestingly include mainly motions of atoms not belonging to the Cu-O planes. For a phonon coupled to an electronic background the Fano profile

$$I(\omega) = I_0 \frac{(\epsilon + q)^2}{(1 + \epsilon^2)} + B(\omega) \quad (1)$$

is generally used to describe the line shape, where $\epsilon = (\omega - \omega_p)/\Gamma$, ω_p is the renormalized phonon frequency that includes all contributions resulting from the interaction of the phonon with elementary excitations, Γ is the linewidth, q is the asymmetry parameter, and $B(\omega)$ is the non-interacting with the phonon part of the electronic excitations continuum. In the case of real phonon and electronic scattering amplitudes t_p and t_e , and a flat scattering background around the phonon frequency

$$\frac{1}{q} = \frac{t_e}{t_p} \pi \rho V, \quad (2)$$

where $\rho(\omega) = \text{const}$ is the density of electronic excitations coupled to the particular phonon, V is the related electron-phonon coupling constant, and the intensity of the interacting

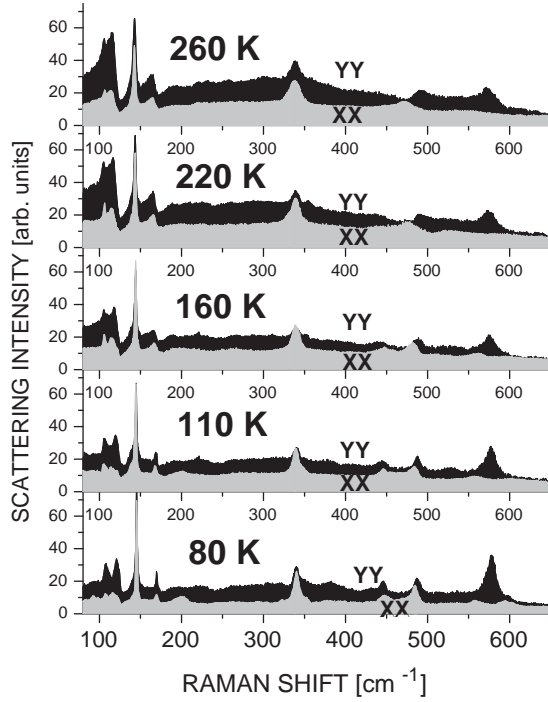


FIG. 5: (Color online) Variation of the electronic background in the $z(XX)\bar{z}$ and $z(YY)\bar{z}$ spectra of Ortho-II between 260 and 80 K.

with the phonon part of the electronic continuum in Eq.(1) can be expressed as $I_0 = \pi \rho t_e^2$. Under the reasonable assumption that t_e , t_p , and V are only weakly dependent on T , the variations with temperature of the absolute value of $1/q$ and I_0 will be governed mainly by $\rho(T)$. Fig. 6 shows in more detail the variations between 260 and 80 K of profile of the Raman line near 485 cm^{-1} , which corresponds to the apex oxygen A_g mode. In contrast to the known results for twin free Ortho-I crystals, the slopes of Fano shaped profiles in the XX and YY spectra of Ortho-II are of opposite sign, which is not surprising if we take into account that $t_p^{xx} \propto \alpha_{xx}$ and $t_p^{yy} \propto \alpha_{yy}$ are of opposite sign for this mode. It is also evident from Fig. 6 that the Raman lines become more symmetric at lower temperature. The Fano fit of the experimental profiles showed that the $1/q$ factor for the XX and YY decreases, respectively, from -0.6 and $+0.8$ at 300 K to -0.2 and $+0.1$ at 80 K. On the other hand, the electronic background $B(\omega, T)$ remains nearly constant between 300 and 200 K but with further cooling decreases significantly between 200 and 100 K (Fig.5). On the basis of considerations above concerning $1/q(T)$ and $I_0(T)$ being governed by $\rho(T)$, one therefore

concludes that with decreasing temperature the density of electronic excitations coupled to this phonon also decreases, concurrently to the decrease of the electronic background $B(\omega, T)$ already noticed. Such a temperature behavior of the electronic Raman scattering is most consistent with an opening of a gap in the electronic excitations as the pseudogap in the underdoped high temperature superconductors.[29, 30, 31] It is worth noting here that the characteristic temperature $T^* \approx 150$ K, below which Opel et al.[25] have observed weak spectral weight loss in the $z(XY)\bar{z}$ spectra of twinned films of $\text{YBa}_2\text{Cu}_3\text{O}_{6.5}$ ($T_c \approx 60$ K), is in the same temperature range.

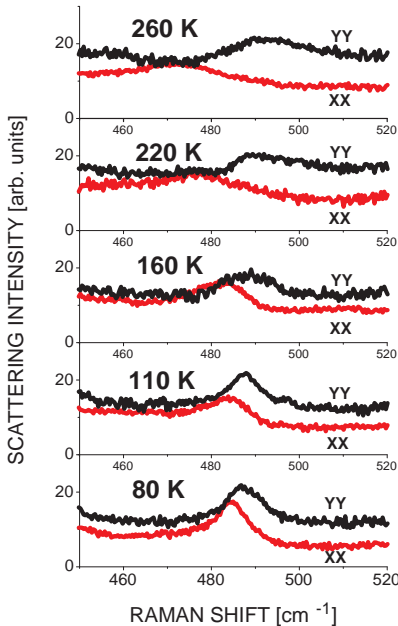


FIG. 6: (Color online) Variation with T of the profile of the Raman line associated with A_g apex oxygen mode.

IV. CONCLUSIONS

The experimental results reported here strongly suggest that some of the previous Raman scattering data[12, 19, 25] obtained from aged twinned surfaces of YBCO_x ($x \approx 6.5$) samples may not be representative of the ordered Ortho-II structure. This study provides more reliable data for identification of the Ortho-II Raman modes, as well as information on the variation of electronic scattering and electron-phonon interactions in the temperature range

where opening of a pseudogap has been claimed.

Acknowledgments

This work is supported in part by the State of Texas through the Texas Center for Superconductivity at the University of Houston (TcSUH) and by the U.S. Air Force Office of Scientific Research (SPRING award ID FA9550-06-1-0401). The work at the University of Sherbrooke has been supported by the National Science and Engineering Research Council of Canada, and the Fonds Québécois de la Recherche sur la Nature et les Technologies.

-
- [1] R. Liang, D. A. Bonn, W. N. Hardy, *Physica C* **336**, 57 (2000).
 - [2] C. Stock, W. J. L. Buyers, Z. Tun, R. Liang, D. Peets, D. Bonn, W. N. Hardy, L. Taillefer, *Phys. Rev. B* **66**, 024505 (2002).
 - [3] C. Stock, W. J. L. Buyers, R. Liang, D. Peets, Z. Tun, D. Bonn, W. N. Hardy, R. J. Birgeneau, *Phys. Rev. B* **69**, 014502 (2004).
 - [4] M. v. Zimmermann, J. R. Schneider, T. Frello, N. H. Andersen, J. Madsen, M. Kall, H. F. Poulsen, R. Liang, P. Dosanjh, W. N. Hardy, *Phys. Rev. B* **68**, 104515 (2003).
 - [5] N. Gedik, J. Orenstein, R. X. Liang, D. A. Bonn, W. Hardy, *Physica C* **408**, 690 (2004).
 - [6] N. Gedik, P. Blake, R. C. Spitzer, J. Orenstein, Ruixing Liang, D. A. Bonn, W. N. Hardy, *Phys. Rev. B* **70**, 014504 (2004).
 - [7] J. Hwang, J. Yang, T. Timusk, S. G. Sharapov, J. P. Carbotte, D. A. Bonn, R. Liang, W. N. Hardy, *Phys. Rev. B* **73**, 014508 (2006).
 - [8] Z. Yamani, B. W. Statt, W. A. MacFarlane, R. X. Liang, D. A. Bonn, W. N. Hardy, *Phys. Rev. B* **73**, 212506 (2006).
 - [9] R. Harris, P. J. Turner, S. Kamal, A. R. Hosseini, P. Dosanjh, G. K. Mullins, J. S. Bobowski, C. P. Bidinosti, D. M. Broun, R. Liang, W. N. Hardy, D. A. Bonn, *Phys. Rev. B* **74**, 104508 (2006).
 - [10] N. Doiron-Leyraud, C. Proust, D. LeBoeuf, J. Levallois, J. B. Bonnemaïson, R. X. Liang, D. A. Bonn, W. N. Hardy, L. Taillefer, *Nature* **447**, 565 (2007).
 - [11] M. Iliev, C. Thomsen, V. Hadjiev, M. Cardona, *Phys. Rev. B* **47**, 12341 (1993).

- [12] O. V. Misochko, S. Tajima, S. Miyamoto, N. Koshizuka, *Solid State Commun.* **92**, 877 (1994).
- [13] M. N. Iliev, V. G. Hadjiev, V. G. Ivanov, *J. Raman Spectroscopy* **27**, 333 (1996).
- [14] E. Faulques, V. G. Ivanov, *Phys. Rev. B* **55**, 3974 (1997).
- [15] M. Iliev, H.-U. Habermeier, M. Cardona, V. G. Hadjiev, R. Gajic, *Physica C* **279**, 63 (1997).
- [16] M. N. Iliev, P. X. Zhang, H.-U. Habermeier, M. Cardona, *Journal of Alloys and Compounds* **251**, 99 (1997).
- [17] M. Osada, M. Käll, J. Bäckström, M. Kakihana, N. H. Andersen, L. Börjesson, *Phys. Rev. B* **71**, 214503 (2005)
- [18] S. I. Bredikhin, G. A. Emelchenko, V. S. Shechtman, A. A. Zhokhov, S. Carter, R. J. Chater, J. A. Kilner, B. C. H. Steele, *Physica C* **179**, 286 (1991).
- [19] D. Palles, N. Poulakis, E. Liarokapis, K. Conder, E. Kaldis, K. A. Müller, *Phys. Rev. B* **54**, 6721 (1996).
- [20] S. Hong, K. Kim, H. Cheong, G. Park, *Physica C* **454**, 82 (2007).
- [21] Y. B. Li, L. F. Cohen, A. D. Caplin, R. A. Stradling, W. Kula, R. Sobolewski, J. L. MacManus-Driscoll, *J. Appl. Phys.* **80**, 2929 (1996).
- [22] K. Conder, *Materials Science & Engineering*, R32, 41 (2000).
- [23] T. Strohm and M. Cardona, *Phys. Rev. B* **55**, 12725 (1997).
- [24] A. Bock, *Ann. Phys. (Leipzig)* **6**, 441 (1999).
- [25] M. Opel, R. Nemschek, C. Hoffmann, R. Philipp, P. F. Müller, R. Hackl, I. Tüttó, A. Erb, B. Revaz, E. Walker, H. Berger, and L. Forró, *Phys. Rev. B* **61**, 9752 (2000).
- [26] T. Devereaux and R. Hackl, *Rev. Mod. Phys.* **79**, 175 (2007).
- [27] M. Krantz and M. Cardona, *J. Low Temp. Phys.* **99**, 205 (1995).
- [28] E. Bascones, T. M. Rice, A. O. Shorikov, A. V. Lukoyanov, and V. I. Anisimov, *Phys. Rev. B* **71**, 012505 (2005); I. S. Elfimov, G. A. Sawatzky, A. Damascelli, arXiv:0706.4276v2 [cond-mat.str-el].
- [29] T. Timusk and B. W. Statt, *Rep. Prog. Phys.* **62**, 61 (1999).
- [30] M. Le Tacon, A. Sacuto, A. Georges, G. Kotliar, Y. Gallais, D. Colson, and A. Forget, *Nature Physics* **2**, 537 (2006).
- [31] V. Hinkov, P. Bourges, S. Pailhes, Y. Sidis, A. Ivanov, C. D. Frost, T. G. Perring, C. T. Lin, D. P. Chen, and B. Keimer, *Nature Physics* **3**, 780 (2007).